Experimental study of the acoustoelectric effects in GaAs-AlGaAs heterostructures

1995 J. Phys.: Condens. Matter 7 7675

(http://iopscience.iop.org/0953-8984/7/39/010)

J. Phys.: Condens. Matter 7 (1995) 7675–7685. Printed in the UK

Experimental study of the acoustoelectric effects in GaAs–AlGaAs heterostructures

J M Shilton, D R Mace, V I Talyanskii†, M Y Simmons, M Pepper, A C Churchill and D A Ritchie

Cavendish Laboratory, University of Cambridge, Madingley Road, Cambridge CB3 0HE, UK

Received 9 July 1995, in final form 24 July 1995

Abstract. We present the results of a detailed experimental study of the electric current and voltage induced in the 2DEG of a GaAs–AlGaAs heterostructure by a surface acoustic wave (SAW). New results are obtained for these acoustoelectric effects at zero and low (< 0.1 T) magnetic fields. At zero magnetic field the acoustoelectric current (voltage) was found to show a non-monotonic temperature dependence with a maximum at 40–50 K. Measurements on high-mobility 2DEGs where the electron mean free path is comparable with the SAW wavelength reveal geometric resonances of the cyclotron orbit with the SAW wavelength. With increasing magnetic field the acoustoelectric effects increase significantly and display rich oscillatory structure. We compare our data for the high-magnetic-field regime with that published in the literature.

1. Introduction

The application of surface acoustic wave (SAWs) to a two-dimensional electron gas (2DEG) has been of great interest recently [1–11]. A SAW propagating in a piezoelectric medium is accompanied by a wave of electrostatic potential, thus permitting the investigation of the interaction of 2D electrons with a travelling electric field wave. The attractive feature of the SAW technique is that the SAW wavelength (λ) can be made sufficiently small ($\lambda = 0.3\ \mu$m has been reported [8]) as to be comparable with the intrinsic lengths relevant to electronic transport in 2DEGs.

Two types of effect due to the interaction between SAWs and 2DEGs have been investigated. The changes in both SAW damping and velocity resulting from this interaction have been studied by several groups [1,5–9]. At low SAW frequency it was shown that the response of 2D electrons to the action of the SAW electric field could be described by the local d.c. 2DEG conductivity, σ_{xx} [1,5]. At higher frequencies the SAW technique was used to measure the deviation of σ_{xx} from d.c. values [6–9]. Willett *et al* [7] measured the dependence of the conductivity on the SAW wave-vector in the fractional-quantum Hall regime at different even-denominator filling factors. The extension of these experiments to SAW frequencies of up to 9 GHz resulted in the discovery of geometric resonances of the cyclotron orbits of the composite fermions with the SAW wavelength [8]. Paalanen *et al* [9] reported that a broad conductivity resonance was observed at about $\omega = 2\pi \times 10^9\ \mathrm{s}^{-1}$, in the small-filling-factor limit, due to the pinning mode of a disordered Wigner crystal.

† Permanent address: Institute of Solid State Physics, Russian Academy of Science, Chernogolovka, Moscow District, Russia.

0953-8984/95/397675+11$19.50

The second class of effects due to the interaction between a SAW and 2DEG are acoustoelectric effects, i.e. the inducement of a direct current or voltage in the 2DEG due to momentum transfer from the SAW to the 2DEG. These effects have been the subject of fewer investigations, and published data are rather contradictory [2–4].

In this paper we present the results of a detailed experimental study of acoustoelectric effects. As we show below, acoustoelectric effects provide a more sensitive method for the study of 2DEG systems than the measurement of SAW damping or velocity change. Unfortunately, SAW-based techniques become less sensitive at low magnetic fields because the high 2DEG conductivity results in screening of the SAW electric field inside the 2DEG. The effective electric field acting on the 2DEG can be expressed in terms of the 2D conductivity σ_{xx} [10]:

$$E_{eff} = \frac{E_{saw}}{1 + \mathrm{i}(\sigma_{xx}/\sigma_m)} \tag{1}$$

where the characteristic conductivity, σ_m, is determined by the SAW velocity and the dielectric permittivity of the substrate. For a (100) GaAs surface and [001] direction of SAW propagation $\sigma_m = 3 \times 10^{-7}\ \Omega^{-1}$ [1,5]. At low magnetic field $\sigma_{xx} \gg \sigma_m$, and so the SAW electric field in the 2DEG is strongly screened. For this reason Willett *et al* [8] did not observe *electron* geometric resonances, whilst the resonances due to the composite fermions were clearly seen. Acoustoelectric effects also decrease with increasing 2DEG conductivity and these effects have not previously been observed in a 2DEG at zero magnetic field. However, in contrast to the measurement of SAW damping or velocity change, in which a small variation in a large quantity must be determined, the use of acoustoelectric techniques merely requires the measurement of a small quantity (the acoustoelectric current or voltage). Moreover, the magnitude of this signal may be increased by increasing the SAW intensity thus making this SAW technique more favourable, particularly in the low-magnetic-field regime where the 2DEG conductivity is high. In this paper we demonstrate that the acoustoelectric current and voltage are indeed sufficiently large for detection, even at zero magnetic field, and the main experimental problem is to eliminate parasitic masking effects.

Two new observations are reported here for the low-magnetic-field regime (< 0.1 T). At zero magnetic field the acoustoelectric current (voltage) was found to have a non-monotonic dependence on temperature revealing a maximum between 40 K and 60 K. This effect was observed in 2DEGs with different mobilities (20 $m^2\ V^{-1}\ s^{-1}$ and 250 $m^2\ V^{-1}\ s^{-1}$ measured at 4 K). At present we have no explanation for this behaviour. For the sample with mobility 250 $m^2\ V^{-1}\ s^{-1}$ we observed non-local effects in the acoustoelectric current (voltage). The acoustoelectric effects were studied at SAW wavelengths of 3 μm, 5 μm and 10 μm which are less than the mean free path in the sample (≈ 20 μm). The experimental dependences of the acoustoelectric current on magnetic field reveal structure which can be explained in terms of geometric resonances of the electron cyclotron orbit with the SAW wavelength.

At higher magnetic fields (> 0.1 T) the acoustoelectric effects increase enormously and display rich structure. We compare our data with other experimental results [2, 3] and with the theory of the acoustoelectric effects developed by Esslinger *et al* [3] and Falko *et al* [10].

2. Experimental technique

A schematic diagram of the sample is shown in the inset of figure 1. A Hall bar with wet-etched mesa, and annealed AuGeNi contacts were defined by standard optical lithography.

Interdigitated transducers (IDTs) for launching and detecting SAWs were fabricated on both sides of the mesa using electron beam lithography, metallization and lift-off. This allows us to launch SAWs in either direction; the induced acoustoelectric current or voltage changes sign as expected. A typical IDT consists of $N = 100$ pairs of fingers 440 μm long. The spatial period of the transducer determines the SAW wavelength, λ. An IDT generates (detects) a SAW in a narrow ($\delta f = f0/N$) frequency range centred around the frequency $f_0 = v/\lambda$, where v is the SAW velocity ($v \approx 2.8 \times 10^3$ m s^{-1} for the [110] direction in GaAs [1, 5]). We used transducers with λ of approximately 10, 5 and 3 μm which correspond to SAW frequencies of approximately 300, 550, and 900 MHz respectively. Samples 1 and 2 were made from a heterostructure with mobility (without illumination) $\mu = 20$ m^2 V^{-1} s^{-1} and carrier density $n = 2.3 \times 10^{15}$ m^{-2} measured at 4 K and samples 3 to 5 from a heterostructure with $\mu = 250$ m^2 V^{-1} s^{-1} and $n = 9.0 \times 10^{14}$ m^{-2}. The IDTs on these samples corresponded to SAW wavelengths λ as follows: samples 1 and 2 ($\lambda \approx 8$ mum); 3 ($\lambda \approx 10$ μm); 4 ($\lambda \approx 5$ μm); and 5 ($\lambda \approx 3$ μm). These devices effectively form a SAW band-pass filter; the frequency characteristic for a typical device (sample 1) is shown in figure 1.

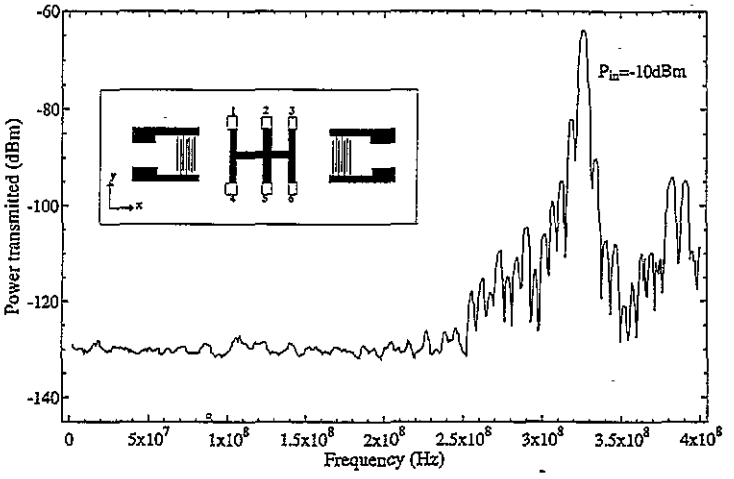

Figure 1. The transmittance characteristic of the SAW delay line taken by a spectrum analyser for sample 1. The SAW wavelength is 8.5 μm, and the input r.f. power is -10 dBm. Inset: schematic of the sample showing the SAW transducers.

To measure acoustoelectric effects we applied amplitude modulated r.f. power to one transducer and detected the corresponding signal using lock-in techniques. The r.f. generator frequency could be swept at the same time in the range 10 to 1350 MHz. We used this facility to check that the signal measured corresponded to the acoustoelectric current (voltage) rather than interference from stray fields induced directly in the 2DEG by the metallization of the transducers (so-called feedthrough or cross-talk). Both the 'open' and 'shorted' [2, 3] geometry were investigated. For open measurements, all the ohmic contacts were left open and longitudinal (between contacts 4 and 6, inset in figure 1) and Hall (between contacts 2 and 5) voltages were measured. In the shorted geometry, longitudinal acoustoelectric current was measured between contacts 4 and 6, and all other contacts were left open.

The influence of the cross-talk signal is clearly seen in figure 2 where we show the dependence of the measured current on frequency. The data shown in the top panel were

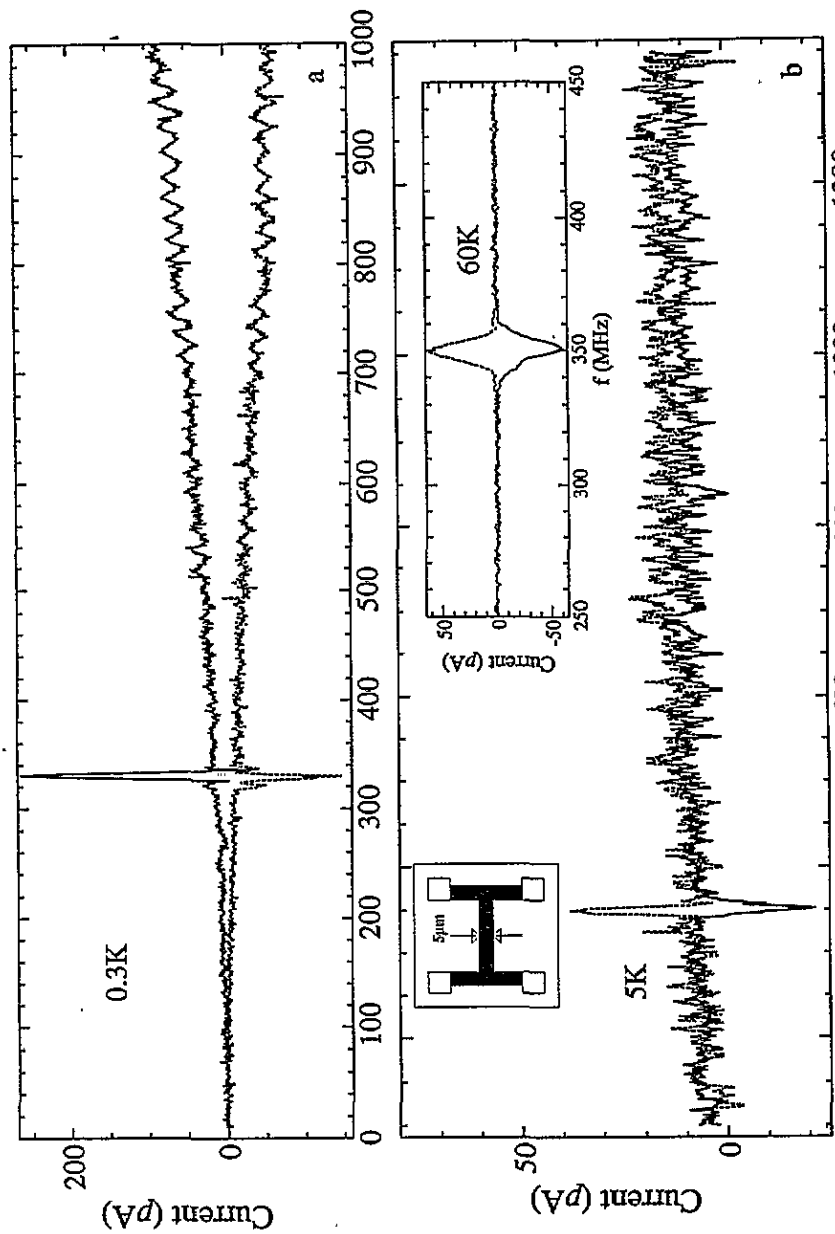

Figure 2. The measured current versus frequency at zero magnetic field. (a) The data for sample 1. Note that the cross-talk signal (like the acoustoelectric current) changes sign with the change of SAW propagation direction. (b) The data for a 5 μm wide and 50 μm long wire (sample 2; $\lambda_{SAW} = 8.1$ μm) shown schematically in the inset. The right-hand inset shows the disappearance of the cross talk signal with increase in temperature.

taken on a mesa 2 mm long and 200 μm wide (shown schematically in the inset of figure 1). The two curves correspond to opposite directions of SAW propagation along the mesa. The peak at 329.5 MHz corresponds to acoustoelectric current, while the broad-band background current is due to rectification of the cross-talk r.f. field. The fact that the cross-talk signal is much smaller than the SAW signal at the transducer resonant frequency is due to careful design of the sample holder. The direction of the acoustoelectric current flow is that which is expected for negatively charged particles being dragged by the SAW. To our knowledge this is the first observation of the acoustoelectric current in a 2DEG at zero magnetic field. The bottom panel in figure 2 shows data taken on a 2DEG wire 5 μm wide and 50 μm long (sample 2). Whilst the acoustoelectric current in the 5 μm wide wire is significantly smaller than the current in the larger mesa, it can still be measured easily. Moreover, the natural assumption that the current is proportional to the width of the wire leads us to the conclusion that acoustoelectric effects can be readily observed in sub-micron mesoscopic 2DEG structures. As the SAW wavelength can be extremely small ($\lambda < 1$ μm, [8]) this technique offers the interesting possibility of studying the response of a mesoscopic structure to the action of a spatially inhomogeneous field.

3. Experimental results and discussion

The remainder of the data presented in this paper were taken with the r.f. generator frequency fixed at the transducers' resonant frequency so that the influence of the cross-talk signal is negligible. In figure 3 we show the temperature dependence of the acoustoelectric current and voltage at zero magnetic field for samples 1 and 3; the geometry of these samples is the same as that shown in the inset in figure 1. Unexpectedly, the acoustoelectric current and voltage show a non-monotonic temperature dependence with a maximum in the region of 50 K (figures 3(a) and 3(b)). The d.c. characteristics of the samples display no peculiarities in this temperature range (figure 4). We monitored the transmission of the SAW (as shown in figure 1) in this temperature range and observed no change in the magnitude of the received SAW signal.

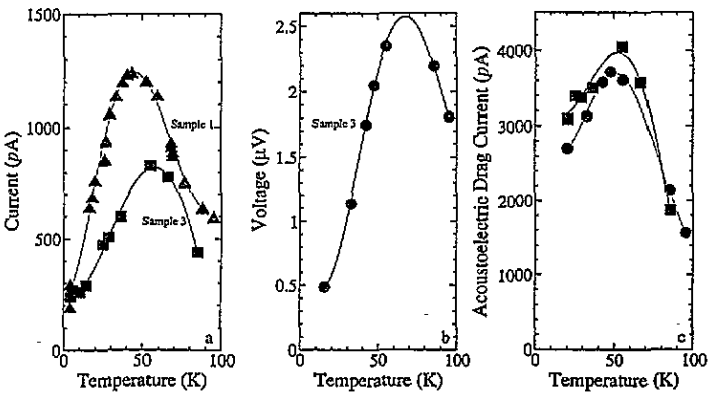

Figure 3. (a) The temperature dependence of the acoustoelectric current for samples 1 ($\lambda_{SAW} = 8.5$ μm) and 3 ($\lambda_{SAW} = 10$ μm) at zero magnetic field. (b) The temperature dependence of the acoustoelectric voltage for sample 3. (c) The calculated temperature dependence of the acoustoelectric drag current for sample 3. Squares are calculated from the data in (a) and circles are calculated from that of (b) (see text).

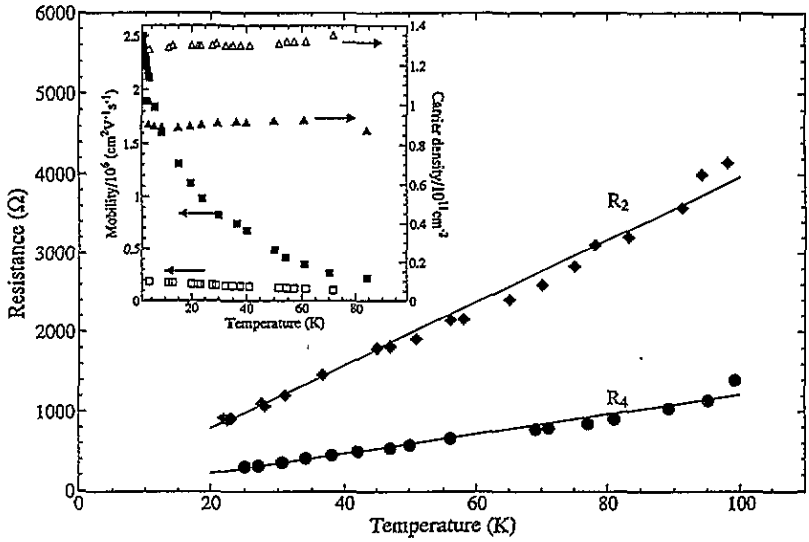

Figure 4. The temperature dependence of the two (R_2) and (R_4) terminal resistances of sample 3. Inset: the temperature dependence of the mobility and carrier density for sample 1 (open symbols) and sample 3 (filled symbols).

To enable comparison of our data with theory, it is necessary to deduce the acoustoelectric drag current density J_{iac} from the measured acoustoelectric current or voltage. The acoustoelectric drag current density may be expressed in the form of a Weinreich relation [12]:

$$J_{iac} = \Lambda_{ix}\frac{I\Gamma}{v} = \Lambda_{ix}Q \tag{2}$$

where $I \propto \exp(-\Gamma x)$ is the acoustic intensity of the wave, Γ is the attenuation due to the 2DEG, the x direction is assumed to be the direction of SAW propagation (figure 1), and Λ_{ix} is the acoustoelectric tensor. The term $Q = I\Gamma/v$ represents the momentum transferred from the SAW to the 2DEG (the 'phonon pressure'). The SAW attenuation can be expressed in terms of 2DEG conductivity as follows [1, 5]:

$$\Gamma = k\frac{K_{eff}^2}{2}\frac{\sigma_{xx}/\sigma_m}{1+(\sigma_{xx}/\sigma_m)^2}. \tag{3}$$

Here, $k = 2\pi/\lambda$ denotes the wave vector of the SAW, and $K_{eff}^2 = 6.4\times10^{-4}$ is the effective electromechanical coupling coefficient of the (100) GaAs surface [1, 5].

The actual current density in the mesa (j_i) differs from that given by equation (2) because the acoustoelectric drag current density (j_{iac}) causes the appearance of a d.c. electric field which in turn causes ohmic current to flow. In the presence of a magnetic field this electric field results in the appearance of a Hall current as well. The following are the equations relating the current densities j_i and j_{iac} in a form which is also applicable when a magnetic field is present [2, 3]:

$$\begin{aligned} j_x &= j_{xac} + \sigma_{xx}E_x + \sigma_{xy}E_y \\ j_y &= j_{yac} + \sigma_{yx}E_x + \sigma_{yy}E_y \end{aligned} \tag{4}$$

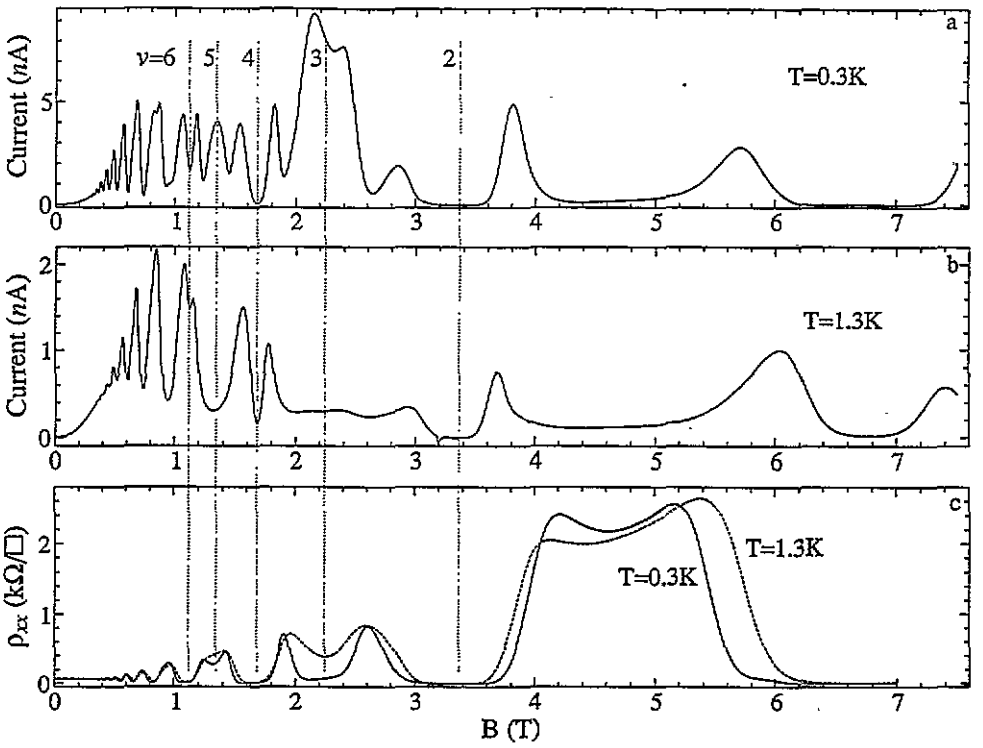

Figure 5. The magnetic field dependence of the acoustoelectric current ((a), (b)) and four-terminal longitudinal resistance (c) for sample 1 at 0.3 K and 1.3 K. The input r.f. power is −15 dBm.

where σ_{ij} are the d.c. conductivities and E_i are the components of the static electric field. The boundary conditions applied to these equations (4) are imposed by the experimental set-up.

When current is measured (using the 'shorted' geometry) the boundary conditions take the form:

$$j_y = 0, \; E_x = 0. \tag{5}$$

If the resistance of the external circuit R_{ext} (including the contact resistance) is non-zero, then the corresponding boundary conditions take the form $I_x = j_x W = E_x L/R_{ext}$ where I_x is the current in the external circuit and L and W are the mesa length and width, respectively.

For the 'open' geometry the boundary conditions are

$$j_x = j_y = 0 \tag{6}$$

and the acoustoelectric voltages can be found, since $V_x = E_x L$, $V_y = E_y W$.

Using these expressions and the data from figure 4 we calculated the acoustoelectric drag current j_{xac} from the measured current and voltage, shown in figures 3(a) and 3(b) respectively; the result is shown in figure 3(c). One can see that the measurements in 'shorted' and 'open geometry' result in the same temperature dependence of the drag current.

Acoustoelectric effects in 2DEGs have been considered theoretically by several authors [3, 10, 11]. In the work of Esslinger *et al* [3] and Falko *et al* [10] the nonlinear mechanism

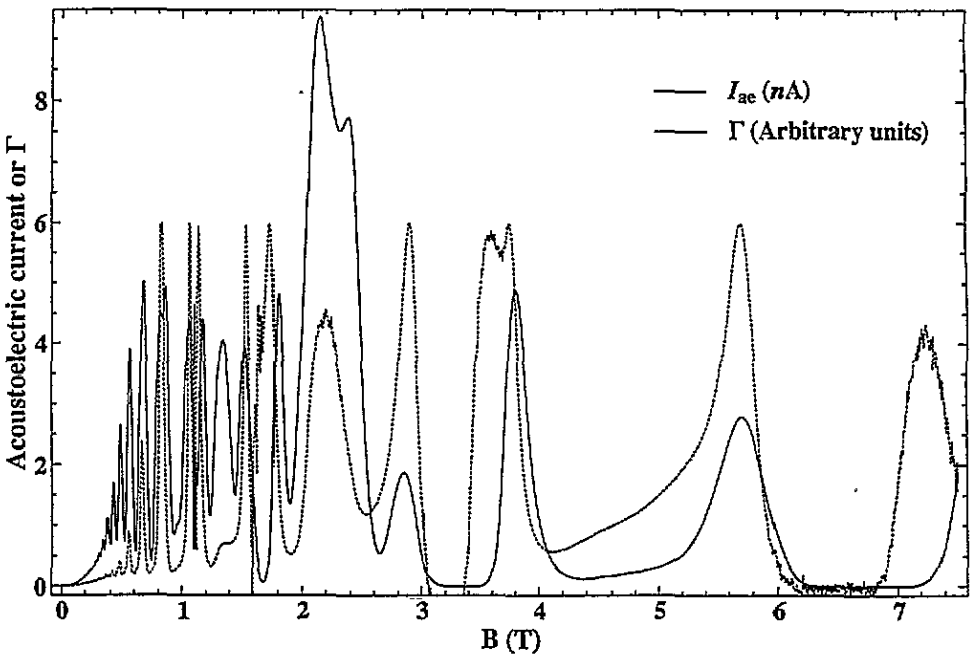

Figure 6. The calculated magnetic field dependence of SAW damping for sample 1 at 0.3 K (dashed curve) shown with the experimental dependence of the acoustoelectric current (solid curve).

leading to acoustoelectric effects was assumed to be the dependence of the conductivity tensor on carrier density, leading to the following expression for the acoustoelectric tensor:

$$\Lambda_{ix} = -\frac{1}{e}\frac{\partial \sigma_{ix}}{\partial n} \tag{7}$$

where n is the electron density and e is the electron charge. Efros and Galperin [11] found $\Lambda_{ix} = (1/e)\sigma_{ix}/n$. Both results, however, converge for vanishing magnetic field. For the temperature range $T < 100$ K, it can be seen from figure 4 that $\sigma_{xx} > 10^{-2}\ \Omega^{-1} \gg \sigma_m = 3 \times 10^{-7}\ \Omega^{-1}$. Thus equation (3) reduces to $\Gamma \alpha \sigma_m/\sigma_x$ such that $j_{xac} \propto (\sigma_{xx}/n)\sigma_m/\sigma_{xx} = \sigma_m/n$. The theoretical scheme outlined above leads us to the conclusion that the acoustoelectric drag current should not change in the temperature range investigated ($T < 100$ K) because the electron density is approximately constant in this temperature range (see the inset in figure 4). The experimental temperature dependence (figure 3(c)) is quite different. A possible explanation for this is the increase in SAW attenuation by bulk phonon scattering, which would effectively reduce the coupling between the SAW and 2DEG [13]. At present, however, we have no definite explanation for this result.

In the presence of a magnetic field the acoustoelectric effects increase enormously and exhibit a rich structure. Figures 5(a) and (b) show the magnetic field dependence of the acoustoelectric current (closed geometry) at 0.3 K and 1.3 K respectively for sample 1. Figure 5(c) shows the corresponding magnetic field dependence of the longitudinal resistance for both temperatures.

It is interesting to compare the structure in the current with that of the 2DEG resistance. Figure 5 shows that the acoustoelectric current does not simply mirror that of the resistance.

Empirically we have found that the current resembles the magnetic field dependence of the SAW attenuation Γ. This is surprising as the link between Γ and the measured acoustoelectric current j_I (given by equations (2), (4) and (5)) is rather complicated. Equation (3) shows that Γ is a non-monotonic function of σ_{xx} with a maximum at $\sigma_{xx} = \sigma_m$. As we traverse a Shubnikov–de Haas minimum, it is possible for the conductivity to pass σ_m twice, thus giving rise to a characteristic double-peak structure in Γ [1, 5]. Figure 6 shows the magnetic field dependence of Γ calculated for sample 1 at $T = 0.3$ K. For comparison, we show on the same picture the magnetic field dependence of the acoustoelectric current (identical to that shown in figure 5(a)). The similarity between the two curves is clearly seen. For even filling factors, where strong Shubnikov–de Haas minima are seen, the double-peak signature is clearest at 0.3 K, although it is still present at 1.3 K, as shown in figures 5(a) and 5(b). At high even filling factors (greater than 6), the acoustoelectric current simply displays maxima because σ_{xx} does not drop below σ_{mm}. No structure is observed at odd filling factors greater than 5 due to the absence of spin-splitting. Our data exhibits more detailed structure than previous experiments [2] probably due to the lower temperature used.

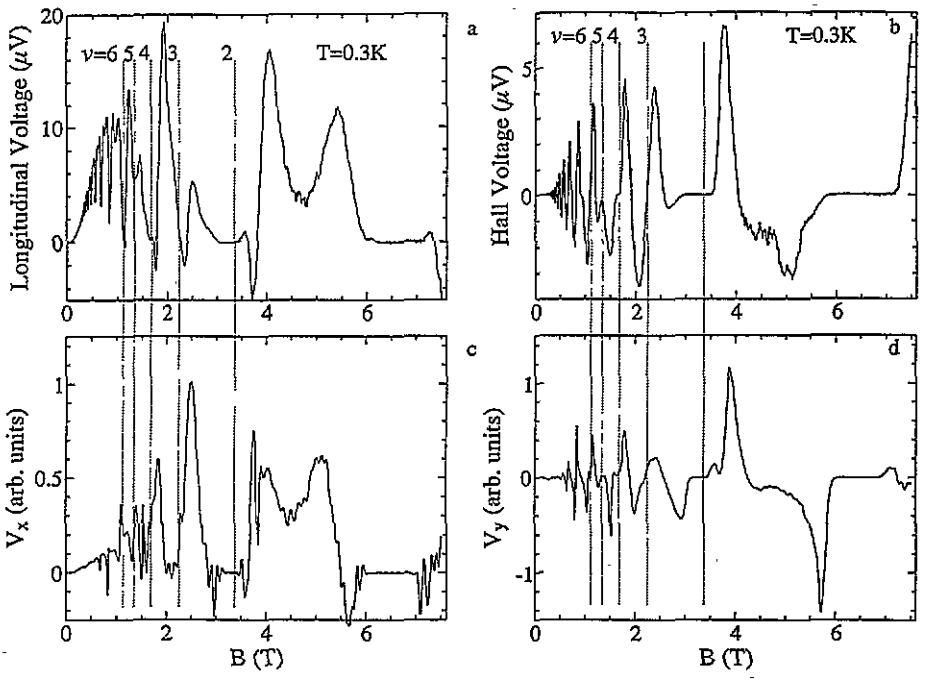

Figure 7. Experimental ((a), (b)) and calculated ((c), (d)) magnetic field dependences of longitudinal and Hall acoustoelectric voltages in 'open' geometry for sample 1. The input r.f. power is −15 dBm.

The experimental results for 'open' geometry are presented in figures 7(a) and 7(b) for sample 1 at 0.3 K. The SAW-induced longitudinal and transverse voltages were measured between contacts 4–6 and 2–5, respectively (see the inset of figure 1). The longitudinal acoustoelectric voltage is zero at integer filling factors, and may be positive or negative, (figure 7(a)) in agreement with data published by Esslinger *et al* [3]. However, we have not observed a double-negative-peak structure around integer filling factors [3] for longitudinal

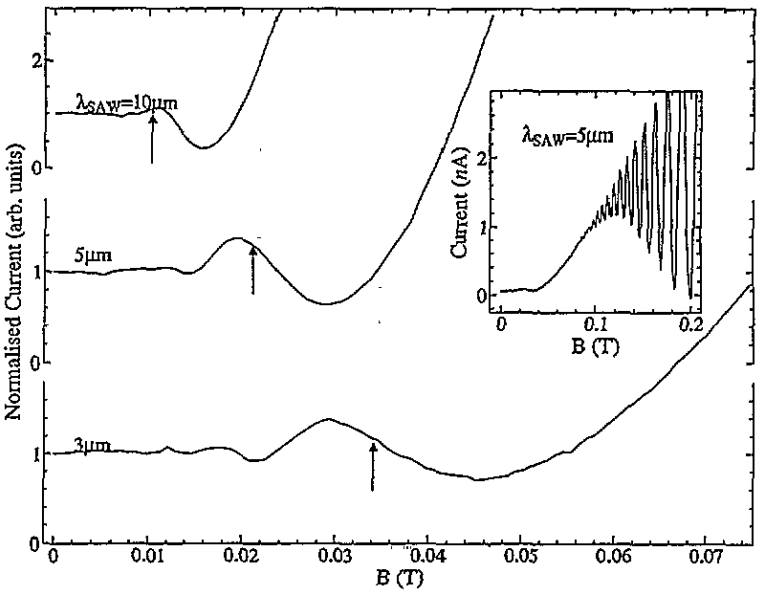

Figure 8. The normalized acoustoelectric current versus magnetic field for different values of SAW wavelength (samples 3 to 5). The temperature is 0.3 K, and input r.f. power is −10 dBm. *Inset: the acoustoelectric current over a larger range of magnetic field; the temperature is 0.3 K,* the input r.f. power is −18 dBm, and $\lambda_{SAW} = 5$ μm (sample 4).

acoustoelectric voltage. Our results for the measurements of the Hall voltage (figure 7(b)) are also similar to those presented by Esslinger *et al* [3].

To calculate the measured acoustoelectric current or voltage from expressions (2) to (7) we need derivatives of σ_{ij} with respect to electron density n at fixed magnetic field B, while from the experimental $R_{xx}(B)$ and $R_{xy}(B)$ data we can extract the derivatives with respect to B at fixed n. The required derivatives can be expressed in the form [3]:

$$\frac{\partial\sigma}{\partial n} = \frac{\partial\sigma}{\partial\nu}\frac{\partial\nu}{\partial n} = \frac{\nu}{n}\frac{\partial\sigma}{\partial\nu}$$

and the problem reduces to finding $\partial\sigma/\partial\nu$ at fixed B. To get these from the experimental $R_{xx}(B)$ and $R_{xy}(B)$ data we shall make the rather arbitrary assumption that σ depends on filling factor ν rather than on n and B separately. The acoustoelectric longitudinal and transverse voltages calculated in this way are shown in figures 7(c) and 7(d). The calculated Hall voltage is in good agreement with that measured, although the agreement is less good for the longitudinal acoustoelectric voltage.

In what follows we would like to discuss briefly the first results on acoustoelectric current measured under nonlocal conditions. More detailed discussion will be given elsewhere. For samples 3 and 5 the mean free path is about 30 μm which is comparable with the SAW wavelengths used. Figure 8 shows the dependence of the acoustoelectric current on magnetic field for low-field values for SAW wavelengths of 3, 5, and 10 μm at 0.3 K. The arrows show the field at which the electron cyclotron diameter coincides with the SAW wavelength. The shift of the structure to higher magnetic field values at lower SAW wavelength unambiguously shows that electron geometric resonances with SAW wavelength are responsible for the structure in the curves. If the temperature is increased to 4 K, the

structure in figure 8 is washed out. To our knowledge this is the first observation of commensurability oscillations for such large cyclotron orbits in 2DEGs. Commensurability oscillations have been previously observed [14–16] in devices in which the carrier density is modulated over a much smaller period (approximately 1 μm) where such long scattering lengths are not required.

In conclusion, we present the results of the first observation of acoustoelectric effects in GaAs–AlGaAs heterostructures under conditions of strong screening. At zero magnetic field an unexpected temperature dependence of the acoustoelectric current was found with a maximum at approximately 50 K. High-mobility 2DEGs are shown to reveal nonlocal acoustoelectric effects. Our results suggest that it may be possible to employ acoustoelectric effects in the study of mesoscopic structures. At sufficiently high magnetic fields acoustoelectric effects show a rich structure. Our data for the 'open' geometry are in qualitative agreement with that published by Esslinger *et al* [3] and can be qualitatively described by the theory formulated therein [3, 10].

Acknowledgments

The authors gratefully acknowledge helpful discussions with E Kogan, C J B Ford and C G Smith. This work was supported by EPSRC.

References

[1] Wixforth A, Kotthaus J P and Weimann G 1986 *Phys. Rev. Lett.* **56** 2104
[2] Esslinger A, Wixforth A, Winkler R V, Kotthaus J P, Nickel H, Schlapp W and Losch R 1992 *Solid State Commun.* **84** 939
[3] Esslinger A, Winkler R V, Wixforth A, Kotthaus J P, Nickel H, Schlapp W and Losch R 1994 *Surf. Sci.* **305** 83
[4] Campbell J W M, Guillon F, D'Iorio M, Buchanan M and Stoner R J 1992 *Solid State Commun.* **84** 735
[5] Wixforth A, Scriba J, Wassermeier M, Kotthaus J P, Weimann G and Schlapp W 1989 *Phys. Rev.* B **40** 7874
[6] Willett R L, Paalanen M A, Ruel R R, West K W, Pfeiffer L N and Bishop D J 1990 *Phys. Rev. Lett.* **65** 112
[7] Willett R L, Ruel R R, Paalanen M A, West K W and Pfeiffer L N 1993 *Phys. Rev.* B **47** 7344
[8] Willett R L, Ruel R R, West K W and Pfeiffer L N 1993 *Phys. Rev. Lett.* **71** 3846
[9] Paalanen M A, Willett R L, Littlewood P B, Ruel R R, West K W, Pfeiffer L N and Bishop D J 1992 *Phys. Rev.* B **45** 11342
[10] Falko V I, Meshkov S V and Iordanskii S V 1993 *Phys. Rev.* B **47** 9910
[11] Efros A L and Galperin Yu M 1990 *Phys. Rev. Lett.* **64** 1959
[12] Weinreich G 1956 *Phys. Rev.* **104** 321; 1957 *Phys. Rev.* **107** 317
[13] The authors would like to thank the referees for pointing out this possibility.
[14] Gerhardts R R, Weiss D and von Klitzing K 1989 *Phys. Rev. Lett.* **62** 1173
[15] Winkler R W, Kotthaus J P and Ploog K 1989 *Phys. Rev. Lett.* **62** 1177
[16] Smith C G, Pepper M, Newbury R, Ahmed H, Hasko D G, Peacock D C, Frost J E F, Ritchie D A, Jones G A C and Hill G 1990 *J. Phys.: Condens. Matter* **2** 3405